ELSEVIER

Performance of sandwich plates with truss cores

Nathan Wicks *, John W. Hutchinson

Division of Engineering and Applied Sciences, Harvard University, Cambridge, MA 02138, USA

Abstract

Sandwich plates with truss cores fashioned from straight struts have distinct advantages relative to other constructions, including those with honeycomb cores. In addition to opportunities afforded by their open architecture, the truss core sandwich plates meet or exceed the load carrying capacity of other competitive constructions. The weight of truss core sandwich plates subject to a crushing stress and arbitrary combinations of bending and transverse shear are optimized subject to buckling and plastic yielding constraints and then compared with the weight performance of other types of optimized plates. Several issues central to the optimization process are addressed by a fundamental model study. These include the relation of designs based on a pure moment loading to those based on combined moment and transverse shear and the accuracy needed to model the various modes of buckling that must be taken into account in the design process.
© 2003 Elsevier Ltd. All rights reserved.

Keywords: Sandwich plates; Truss cores; Optimal design; Buckling; Plastic yielding

1. Introduction

New focus on sandwich plates with truss cores has been motivated by potential multifunctional applications that exploit their open architecture as well as their apparent superior strength and stiffness (Evans et al., 2001). Moreover, new methods have been devised which permit ''micro'' plates with truss cores to be manufactured (Brittain et al., 2001). In the present context the terminology ''truss core'' refers to a core constructed from beam elements but not folded plates, as is sometimes implied. A preliminary study (Wicks and Hutchinson, 2001) has revealed that the perfor-

mance of optimized sandwich plates with truss cores is competitive with more widely used constructions, including sandwich plates with honeycomb cores and stringer stiffened plates. A more extensive study of the performance of optimized truss core sandwich plates is undertaken in the present paper. We begin by investigating the optimal design of a model of a two-dimensional truss structure subject to pure bending (see Fig. 1). The various buckling modes of this structure can be analyzed exactly, providing insights into the validity of the approximations that are usually invoked in the optimal design of more complicated structures such as truss core sandwich plates. The model problem also reveals the connection between an optimal configuration designed to carry a pure moment and its counterpart designed to carry
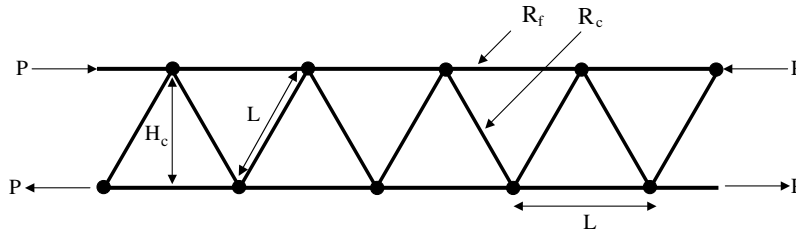
Fig. 1. Geometry of the two-dimensional infinite model truss.

a combination of moment and transverse shear force. The second part of the paper specifically addresses the optimization of sandwich plates with truss cores subject to a crushing stress, bending, and transverse shear. The optimal configurations are compared to optimized plates with honeycomb cores.

2. A two-dimensional truss under pure moment

The infinite truss shown in Fig. 1 carries a moment $M = PH_c$. Each member is taken to have a solid circular cross section, with radius R_f for the horizontal members and radius R_c for the inclined core members. All members are made from the same material whose Young's modulus is E and initial yield stress in tension is σ_Y. All members have length L such that each triangular group is equilateral and $H_c = \sqrt{3}L/2$. Individual truss members are assumed to be slender (i.e. $R/L \ll 1$) and they are regarded as beam columns. At the joints, the members are assumed rigidly connected to one another such that ends of each member meeting at a joint undergo the same displacements and rotation. Only in-plane deformations are considered.

2.1. Bifurcation buckling analysis: exact formulation

The analysis reveals all possible bifurcation buckling modes of the truss and the associated critical moments. Two distinct modes of importance emerge: a mode with sinusoidal half-wavelength equal to the member length wherein compressed members buckle between their joints and a longer wavelength mode.

As is customary in investigations of this kind, the pre-buckling load is approximated as being carried entirely by the horizontal members. This is an excellent approximation since the axial forces in the core members are zero and the elastic energy induced by bending in the pre-buckling response is extremely small. The bifurcation buckling analysis is given in Appendix A. Each member is represented as a beam column, and its deformation is expressed in terms of the displacement components and rotation at its ends where it connects to adjoining members. The eigenvalue problem for the bifurcation mode is formulated exactly as an infinite set of finite difference equations involving the joint displacements and rotations. The equations admit sinusoidal solutions with a wavelength λ. With $M_c(\lambda)$ denoting the minimum eigenvalue at a given λ, the critical moment governing bifurcation is the lowest value of $M_c(\lambda)$ over the entire spectrum of λ. The full spectrum of eigenvalues is spanned for the range of wavelengths, $1 \leqslant \lambda/(2L) < \infty$, as discussed in Appendix A.

Examples of the eigenvalue spectrum are plotted in Fig. 2. In the example with the larger ratio, R_c/R_f, the lowest eigenvalue is associated with the short wave mode ($\lambda = 2L$), corresponding to buckling of the compressed horizontal members between their joints, as depicted. The other eigenvalue spectrum shown is for very slender core members relative to the horizontal members. In this example, the lowest eigenvalue is associated with a longer wave mode ($\lambda \approx 3.6L$). This longer wave mode appears when the ratio, R_c/R_f, is very small, as will be quantified in the next section. The result from the approximate formula for the short wave eigenvalue that is presented in Section 2.2 very accurately predicts the value plotted at $\lambda = 2L$ for both of the R_c/R_f values shown in Fig. 2.
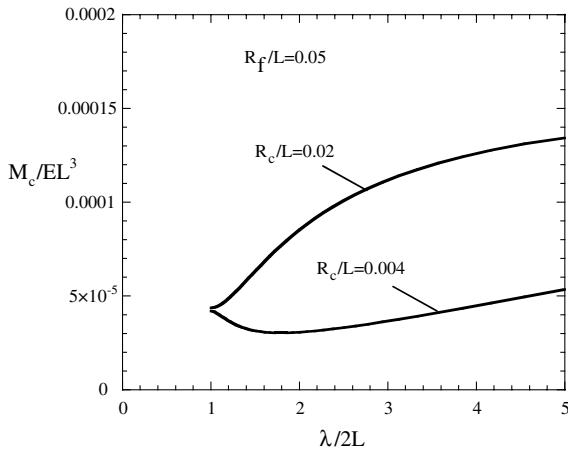
Fig. 2. Eigenvalue spectrum, $M_c(\lambda)$, for $R_f/L = 0.05$, for two core radius values ($R_c/L = 0.02$ and $R_c/L = 0.004$).

2.2. Approximate results for short and longer wavelength buckling modes

The model problem is sufficiently simple such that it is possible to use results from the exact analysis to carry out an optimal design of the truss, and this will be done. The primary aim in conducting the model study, however, is to make use of the exact solution to assess the validity of using approximate formulas for the two buckling modes highlighted above. Optimal design of more complex structures under more general loads will generally employ approximate formulas of the type that will be introduced below. Thus, the present model problem affords an opportunity to quantitatively evaluate the accuracy of optimal configurations obtained using approximate buckling formulas.

The scheme for estimating the constraining effect of the lower portion of the structure on the bucking of the horizontal members in the *short wavelength mode* is depicted in Fig. 3a. The top compression member is constrained to have zero deflection at each joint and its rotation is constrained by a torsional spring. The spring constant is determined from the problem depicted in Fig. 3b where a moments of equal magnitude but alternating sign act on the remaining part of the truss. If the effect of the tensile load P on the bottom
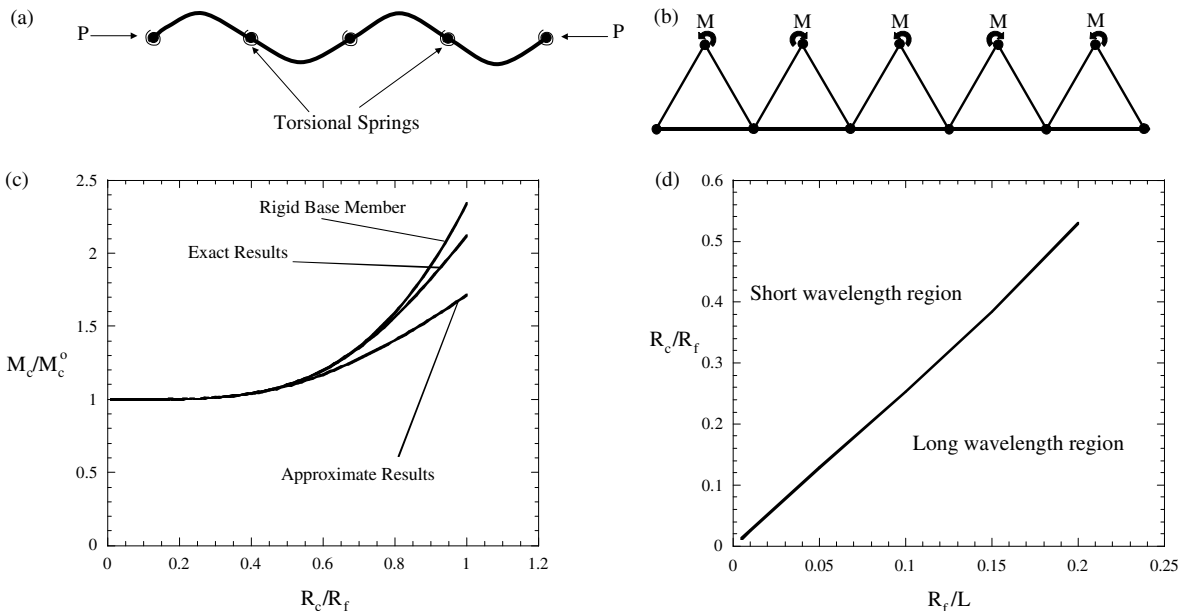
Fig. 3. Approximate analysis of the short wavelength buckling mode (a)–(c) and the border between the long and short wavelength buckling (d).

horizontal member is neglected, the torsional spring constant can be determined exactly as

$$K = M/\theta = \frac{8EI_c}{L}\left\{1 + \frac{16}{3}q^2 + \frac{8}{3}\frac{I_c}{I_f}\left(\frac{3}{4} - q\right)^2\right\}^{-1}$$

$$q = \frac{3I_c}{8I_f + 4I_c} \tag{1}$$

where $I_f = \pi R_f^4/4$ and $I_c = \pi R_c^4/4$. If the horizontal members are much thicker than the core members such that $q \cong 0$, then $K = 8EI_c/L$, and this is identical to the case where the core members are attached to a rigid foundation. The eigenvalue equation for the critical load P for an infinite beam having zero deflection and constrained by the above torsional spring at equally spaced distances L is

$$\sqrt{\frac{P}{EI_f}}\frac{L}{2}\cot\left(\sqrt{\frac{P}{EI_f}}\frac{L}{2}\right) = -\frac{KL}{4EI_f} \tag{2}$$

By expanding (2) in a Taylor series about $\sqrt{P/EI_f}L = \pi$ (appropriate for sufficiently small KL/EI_f) and retaining up to and including terms of second order, one obtains the explicit approximation for the short wavelength buckling load

$$\sqrt{\frac{P}{EI_f}}\frac{L}{2} = \frac{\pi}{4} + \sqrt{\left(\frac{\pi}{4}\right)^2 + \frac{KL}{4EI_f}} \tag{3}$$

Results for the critical buckling moment from the exact analysis are compared in Fig. 3c with results from (3) for the full expression (1) for K, and the two sets are in good agreement for values of R_c/R_f up to about 0.5. In this figure, M_c^0 denotes the critical moment with $K = 0$ corresponding to simple support of a beam of length L. An even better approximation is seen to pertain for the case where the base horizontal members are taken to be rigid, i.e. $K = 8EI_c/L$.

The lowest eigenvalue is associated with a "long" wavelength mode only when R_c/R_f becomes smaller than a transitional value. Fig. 3d is a plot of the transition value of R_c/R_f as a function of R_f/L at which the long wavelength mode has the same eigenvalue (buckling moment) as the short wavelength mode ($\lambda = 2L$). The condition that ensures that the short wavelength mode is critical is well approximated by

$$\frac{R_c}{R_f} \geqslant -0.00313 + 2.62\frac{R_f}{L} \tag{4}$$

An approximate approach to estimating the critical load associated with the "long" wavelength mode has the compressed beam resting on an elastic foundation where the spring constant for normal displacement is obtained for triangular core elements rigidly supported at the bottom beam. The critical load from such an analysis is $P = 2\sqrt{EI_fS}$, where the spring constant is $S = 2H^2R_c^2\pi E/L^4$. Equating this critical load with the short wavelength critical load based on simple support at the nodes gives the approximation to the transition as $R_c/R_f = \pi^2R_f/2\sqrt{6}L = 2.01R_f/L$. The error in this result compared to the transition (4) is due to the fact that the so-called long wavelength mode, in fact, is not really long compared to the member length.

In the optimization described below for a pure moment loading, condition (4) will be invoked as a constraint on the design. It is conceivable that a lighter weight design might be attained if R_c/R_f were allowed to become even smaller. However, as we shall see, the inclusion of any realistic level transverse shear in the design process ensures that R_c/R_f is well above the transition ensuring that short wavelength buckling is critical.

2.3. Optimization of the two-dimensional truss subject to pure moment

The dimensions of the truss members, R_c, R_f and L, are now identified that give the lightest weight given that the truss must support a prescribed moment M such that the force carried by the horizontal members is $P = 2M/\sqrt{3}L$. With w as the weight per unit volume of the material comprising the members, the weight per unit length of the truss is $W = 2\pi w(R_c^2 + R_f^2)$. The horizontal members must not exceed yield requiring, $\sqrt{3}\pi\sigma_Y R_f^2 L/2 \geqslant M$, while the short wavelength (3) and long wavelength (4) buckling conditions provide the respective constraints

$$\frac{\sqrt{3}}{2}\pi\left(\frac{\pi}{4} + \sqrt{\left(\frac{\pi}{4}\right)^2 + \frac{KL}{4EI_f}}\right)^2 \frac{ER_f^4}{L} \geqslant M$$

and

$$\frac{R_c}{R_f} \geqslant -0.00313 + 2.62\frac{R_f}{L}$$

Plastic buckling of the horizontal members is not explicitly considered since it is excluded by the constraint on plastic yielding. The yielding constraint could be replaced by a constraint on plastic buckling, but this would have relatively little influence on the optimal design. Except for materials with very high strain hardening, the plastic buckling load is only slightly higher than the load at plastic yield and for this reason the constraint on plastic yielding is only slightly conservative.

The only length quantity other than unknown member dimensions is $(M/E)^{1/3}$. To put the optimization problem in non-dimensional form, introduce dimensionless member variables as $\vec{x} \equiv (x_1, x_2, x_3) = (R_f, R_c, L)/(M/E)^{1/3}$. The dimensionless optimization problem requires that the dimensionless weight, $W/[w(M/E)^{2/3}] = 2\pi(x_1^2 + x_2^2)$, be minimized with respect to $\vec{x}$ subject to the three constraints noted above, i.e.

$$\frac{\sqrt{3}\pi}{2}\varepsilon_Y x_1^2 x_3 \geqslant 1$$

$$\frac{\sqrt{3}\pi^3}{8}\left(\frac{1}{2} + \sqrt{\frac{1}{4} + k}\right)^2 x_1^4 x_3^{-1} \geqslant 1 \qquad (5)$$

$$\frac{x_2}{x_1} \geqslant -0.00313 + 2.62\frac{x_1}{x_3}$$

Here, $\varepsilon_Y = \sigma_Y/E$ is the yield strain and k is

$$k = \frac{KL}{\pi^2 EI_f} = \frac{4}{\pi^2}(x_2/x_1)^4\frac{(x_2/x_1)^4 + 2}{2(x_2/x_1)^4 + 1}$$

The yield strain is the only parameter in the dimensionless optimization problem. For a numerical example, take $\varepsilon_Y = 0.007$ corresponding to a high strength aluminum considered in the earlier study (Wicks and Hutchinson, 2001). The solution to the optimization problem is

$$x_1 = 1.4088, \quad x_2 = 0.19249$$
$$x_3 = 26.457, \quad W/[w(M/E)^{2/3}] = 12.703 \qquad (6)$$

All three constraints in (5) are active for the solution.

3. The optimal two-dimensional truss subject to both moment and transverse shear force

Now suppose the same truss at its most severely loaded section carries a moment M and a shear force V. Let $\ell = M/V$ and assume that $\ell \gg L$, which necessarily holds if the truss contains multiple sections. (A cantilever beam of length ℓ loaded with a force V at its free end experiences the moment $M = V\ell$ at its supported end.) The most heavily loaded core members are subject to forces $\pm 2V/\sqrt{3}$, depending on their inclination and the direction of the shear force, while the most heavily loaded horizontal members are subject to $2M/(\sqrt{3}L)$.

With M and V prescribed, the truss weight is to be minimized by selecting R_c, R_f and L subject to the three constraints imposed in Section 2.3 (long and short wavelength buckling and yield of the horizontal members) plus an additional two constraints: buckling and yield of the core members. The prior discussion of plastic buckling being excluded by the constraint on plastic yielding applies here as well. Now, the long and short wavelength buckling conditions for the compressed horizontal members are clearly approximate because the moment and, therefore the axial load, vary from member to member. As is customary in optimization studies, the conditions are nevertheless assumed to apply "locally". This approach is appropriate for a slender structure with $\ell \gg L$ for which the axial forces will change by a small amount from member to member. Since the design is based on the maximum moment carried by the structure, this approach will underestimate the buckling loads and lead to a conservative design. A set of dimensionless variables different from that employed above is used: $\vec{x} \equiv (x_1, x_2, x_3) = (R_f, R_c, L)/\ell$. With this choice, $W/(w\ell^2) = 2\pi(x_1^2 + x_2^2)$ must be minimized with respect to $\vec{x}$ subject to the five constraints

$$\frac{\sqrt{3}\pi^3}{8}\left(\frac{1}{2} + \sqrt{\frac{1}{4} + k}\right)^2 x_1^4 x_3^{-1} \geqslant \Omega$$

(short wavelength buckling)

$$\frac{x_2}{x_1} \geqslant -0.00313 + 2.62\frac{x_1}{x_3}$$

(long wavelength buckling)

$$\frac{\sqrt{3}\pi}{2}\varepsilon_Y x_1^2 x_3 \geqslant \Omega \quad \text{(face sheet yielding)}$$

$$\frac{\sqrt{3}\pi^3}{2} x_2^4 x_3^{-2} \geqslant \Omega \quad \text{(core buckling)} \qquad (7)$$

$$\frac{\sqrt{3}\pi}{2}\varepsilon_Y x_2^2 \geqslant \Omega \quad \text{(core yielding)}$$

Now there are two-dimensionless parameters in the problem, ε_Y and the dimensionless load combination, $\Omega = V^3/(EM^2)$. The core members are taken as clamped at the ends in evaluating their elastic buckling loads, consistent with the optimal outcome wherein the truss has face members which are more than twice as thick as the core members.

The solution to the optimization problem can be determined with a nonlinear optimization routine such as that available in the IMSL Library for numerical analysis. For $\varepsilon_Y = 0.007$, the dimensionless weight of the optimal truss is plotted against $V/(EM^2)^{1/3}$ in Fig. 4a, while the member dimensions for the optimal truss are shown in Fig. 4b, c and d. This plot spans the entire range of loading for which the truss can be regarded as being a relatively slender beam. Note that at the largest value of $V/(EM^2)^{1/3}$ shown, L/ℓ is 0.20. The constraints active over the entire range plotted are short wavelength buckling, yield of faces, and elastic buckling of the core members. The aspect ratio of the core members is such that the long
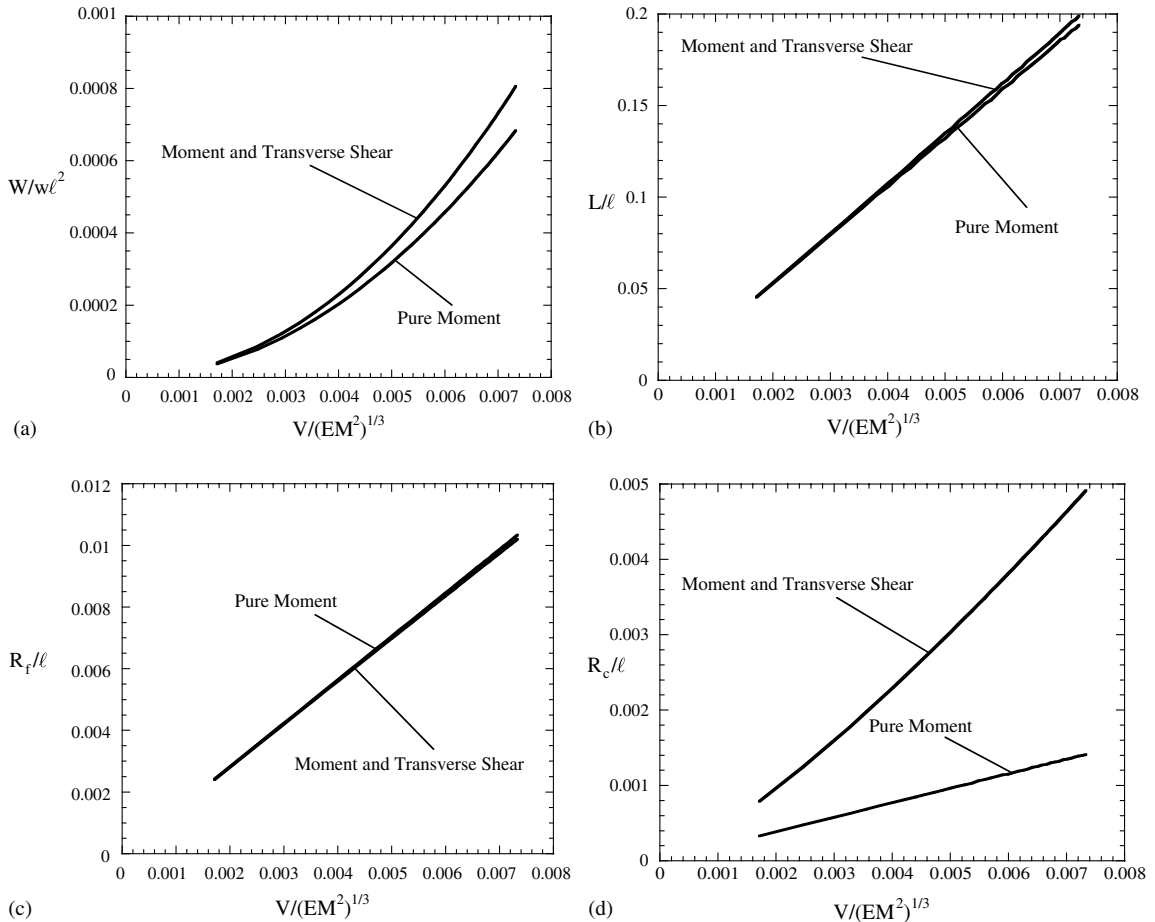
Fig. 4. Weight per unit length (a) and member dimensions (b)–(d) for optimally designed two-dimensional truss carrying moment M and shear force V for $\varepsilon_Y = 0.007$. The results for the truss designed to carry a pure moment M are also included for comparison.

wavelength buckling mode is not at issue (i.e. the left hand side of second constraint in (7) greatly exceeds the right hand side).

The dimensionless results for the pure moment problem in (6) can be re-expressed in terms of the non-dimensional variables used in (7) and in Fig. 4 as

$$\frac{W}{w\ell^2} = \Omega^{2/3} \frac{W}{w(M/E)^{2/3}}$$
$$(R_f, R_c, L)/\ell = \Omega^{1/3}(R_f, R_c, L)/(M/E)^{1/3}$$ (8)

In this form, V is an inessential parameter that appears in the normalization on both sides of the equations in the same manner. Thus, the results for the truss optimized under a pure moment can be directly compared with the optimal truss designed to carry both moment and transverse shear force, and that comparison is included in the several parts of Fig. 4. Even when the shear force is very small, the pure moment design always underestimates the weight of a truss designed to carry both moment and shear force, although the error in weight is not very large. More significantly, the member dimensions of the truss designed to carry only a pure moment are very different from those based on the combined load design. While the optimal dimensions for L/ℓ and R_f/ℓ are comparable for the two cases, the pure moment analysis underestimates R_c/ℓ by as much as 400% compared to the combined load analysis over the load range plotted.

The optimal values of R_c/R_f for the combined moment and transverse shear case are all well within the range where the short wave buckling mode is the lowest buckling eigenvalue, as already emphasized. A lower weight design under pure moment optimization might exist if the constraint requiring the short wavelength mode to be critical were relaxed. This would hardly be worth pursuing given that essentially any transverse load applied to the structure excludes the possibility of the long wavelength mode. Sizing the core members to carry the transverse shear ensures that they are sufficiently substantial such that the long wavelength mode does not occur. For the two-dimensional truss beam, at least, a optimal design based on a pure moment appears to lead to a structure

which is inadequate even when very small transverse shear loads are applied.

4. Optimization of sandwich plates with truss and honeycomb cores

Optimizations of sandwich plates with truss cores and with honeycomb cores have been performed previously (Wicks and Hutchinson, 2001). In this section we optimize sandwich plates with truss cores subject to bending, transverse shear, and a crushing stress, as shown in Fig. 5. A more accurate approximation for the critical buckling stress of the face sheets than that employed earlier is introduced in this paper. A similar optimization is also performed for a honeycomb core sandwich plate to provide a weight performance comparison.

As in the examples discussed above, the design focuses on uniform plates even though for specific load distributions a tapered plate might be more weight efficient. The objective in this paper is to uncover the relative performance of truss core sandwich plates relative to honeycomb construction. More efficient designs might also make use of distinct materials for the core and faces. Here, to limit the possibilities, we restrict attention to a common material with weight density w for all core members and face sheets. The tetragonal truss core is comprised of tripods whose members all have length L_c and a solid circular cross-section of
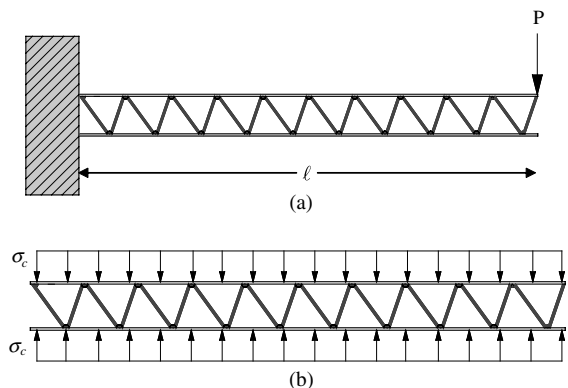
Fig. 5. Loading situation for panels under transverse loading (a) and crushing stress (b).

radius R_c. The weight per unit area of a plate with truss core and solid face sheets is

$$W = 2w \left[t_f + \frac{\pi}{\sqrt{3}} \frac{L_c R_c^2}{L_c^2 - H_c^2} \right] \qquad (9)$$

with t_f as the face sheet thickness and H_c as the core thickness. Conventions for the tetragonal core structure are shown in Fig. 6a and b. The honeycomb core is a regular hexagon with height H_c (the core thickness), web thickness t_c, and web length L_c. The weight per unit area of sandwich plate with the honeycomb core is

$$W = 2w \left[t_f + \frac{H_c t_c}{\sqrt{3} L_c} \right] \qquad (10)$$

where t_f is the thickness of each face sheet. The conventions for the honeycomb cores are shown in Fig. 6c.

The performance of tetragonal and honeycomb cores under shear and compression are of particular interest in sandwich plate design. Key design properties of the two cores are the elastic shear modulus, the crushing strength (both yield and elastic buckling), and shear strength (again, both yield and elastic buckling). These properties are tabulated in Fig. 7a, expressed in terms of the relative density (ρ_c) of the core defined as the volume of core material per volume of core. The properties in Fig. 7a are for a regular tetragonal core ("regular" meaning that the distance between nearest nodes on the face sheets is the same as the core member length, or $H_c/L_c = \sqrt{2/3}$). Of particular relevance is the scaling of the elastic buckling properties of these cores. For the tetragonal core, the buckling strength scales with the core relative density squared. For the honeycomb core, the buckling strength scales with the core relative

	Tetragonal Core	Honeycomb core
Elastic shear modulus	$\bar{G} = \frac{1}{9} E \rho_c$	$\bar{G} = \frac{1}{3(1-v^2)} E \rho_c$
Crushing strength (plastic yield)	$\bar{\sigma} = \frac{2}{3} \sigma_Y \rho_c$	$\bar{\sigma} = \sigma_Y \rho_c$
Crushing strength (elastic buckling)	$\bar{\sigma} = \frac{\sqrt{2}\pi}{9} E \rho_c^2$	$\bar{\sigma} = \frac{\pi^2}{4(1-v^2)} E \rho_c^3$
Shear strength (plastic yield)	$\bar{\tau} = \frac{1}{3\sqrt{2}} \sigma_Y \rho_c$	$\bar{\tau} = \frac{2}{3\sqrt{3}} \sigma_Y \rho_c$
Shear strength (elastic buckling)	$\bar{\tau} = \frac{1}{18} E \rho_c^2$	$\bar{\tau} = \frac{\pi^2 k_s}{24(1-v^2)} E \rho_c^3$

(a)

(b)

Fig. 6. Conventions for tetragonal (a)–(b) and honeycomb (c) core structures. Transverse load lines are parallel to $A - A'$. In (b) solid core nodes are at the upper face sheet, and open nodes are at the lower sheet.
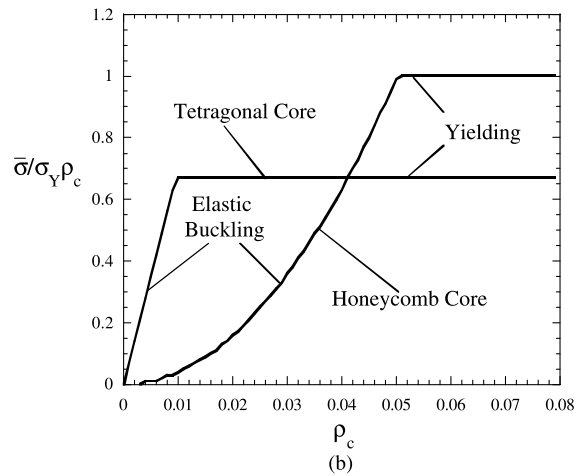
Fig. 7. Table of properties of regular tetragonal and honeycomb core sandwich panels (a). Crushing strength of regular tetragonal and honeycomb core sandwich panels as a function of relative density (b).

density cubed. To illustrate the importance of this factor, the crushing strength properties of both cores as a function of core relative density have been plotted for a representative yield strain of 0.007 in Fig. 7b. For low density cores, typical of those used in sandwich plates, the tetragonal core is significantly stronger. This observation points to the potential advantage of tetragonal core structures for use in sandwich panels.

4.1. Sandwich plate with truss or honeycomb core

The general situation envisioned is again that of a uniform, infinitely wide plate subject to a maximum moment per unit length M and a maximum transverse shear force per unit length V. Bending occurs only about the direction parallel to the loading line. A wide plate under three-point loading with force per unit length $2P$ at the center is a prototypical example. Each half of the plate carries a uniform transverse shear load per length, $V = P$, and a maximum moment per length, $M = P\ell$, at the center, where ℓ is the half-length of the plate. In this example, the maximum moment and the maximum shear transverse force are attained at the same point, but that is not essential nor to be expected. In the general situation, the ratio of the maximum moment to the maximum transverse force (both per unit length),

$$\ell \equiv \frac{M}{V}$$

defines a quantity with dimensions of length which is central in the analysis. The study is limited to relatively thin plates in the sense that the thickness, H_c, is assumed to be small compared to ℓ. Thus, L_c, the core member length, will also be small compared to ℓ.

The four constraints in the optimization under moment and transverse shear are face sheet yielding, face sheet buckling/wrinkling, core member yield, and core member buckling. In this study, a constraint on crushing strength is also included because sandwich plates optimized without this constraint tend to be susceptible to crushing. This is especially true for honeycomb core plates. Consider a plate subject to a uniform crushing stress σ_c, as shown in Fig. 5. The tetragonal core

member forces due to this crushing stress are $\sqrt{3}\sigma_c L_c d^2 / 2H_c$ where $d = \sqrt{L_c^2 - H_c^2}$.

This crushing stress adds two more strength constraints to the optimization—core member yielding and buckling under crushing stress. The six constraints are thus

$$\frac{M}{t_f H_c} \leqslant \sigma_Y \quad \text{(face sheet yielding)}$$

$$\frac{M}{t_f H_c} \leqslant \frac{4E}{27(1-v^2)}\left(\frac{t_f}{d}\right)^2\left(\frac{\pi}{4} + \sqrt{\left(\frac{\pi}{4}\right)^2 + \frac{9(1-v^2)d}{4Et_f^3}\kappa}\right)^2$$

(face sheet buckling)

$$\text{where } \kappa = \frac{\pi E R_c^4}{4\sqrt{3}L_c d}\left(12 - \frac{6d^2}{L_c^2}\right) + \frac{\pi G R_c^4}{4\sqrt{3}L_c d}\left(\frac{3d^2}{L_c^2}\right)$$

$$\frac{\sqrt{3}VdL_c}{H_c \pi R_c^2} \leqslant \sigma_Y \quad \text{(core member yielding)}$$

$$\frac{\sqrt{3}VdL_c}{H_c \pi R_c^2} \leqslant \frac{\pi^2 E R_c^2}{L_c^2} \quad \text{(core member buckling)}$$

$$\sigma_c \leqslant \frac{2\sigma_Y \pi R_c^2 H_c}{\sqrt{3}L_c d^2} \quad \text{(core member crushing yield)}$$

$$\sigma_c \leqslant \frac{2\pi^3 E R_c^4 H_c}{\sqrt{3}L_c^3 d^2} \quad \text{(core member crushing buckle)}$$

(11)

The elastic buckling stress of the compressed face sheet is associated with a sinusoidal mode varying only in the compression direction with nodes at the lines where the joints of the core tripods are attached to the face sheets. The κ factor above is used to model the rotational resistance of the core tripods on the face sheets at the nodes. This factor assumes that these tripods are clamped at the lower (tensile) face, based on the accuracy of the equivalent assumption in the earlier 2D problem (see Fig. 3b). No "long wavelength" constraint is present due to the results of the earlier 2D problem—the other core constraints (core yield and buckling) size the core members such that the long wavelength modes are suppressed. These buckling constraints for the core members are valid for members assumed to be clamped at the face sheets.

The weight per unit area and constraints are written in dimensionless form using $\ell = M/V$ and the four design variables $\vec{x} = (t_f/\ell, R_c/\ell, H_c/\ell, d/\ell)$.

The normalized weight per unit area, $W/w\ell$, and the six dimensionless constraints involve only the parameters: σ_Y/E (taken as 0.007 in the calculations), v (taken as $1/3$ in the calculations), $V/\sqrt{EM}$, and the normalized crushing strength, σ_c/σ_Y. The solution to this optimization problem was again found using an IMSL subroutine. The details of the honeycomb core analysis can be found in the earlier study on this topic (Wicks and Hutchinson, 2001).

4.2. Optimization with no constraint on the crushing stress

The fully optimized (minimum weight) results for these structures in the absence of any constraint on crushing stress is shown in Fig. 8a. The plots are terminated at $V/\sqrt{EM} \cong 0.0018$, as larger values of $V/\sqrt{EM}$ generate plates that would not be considered thin, and thus the range of $V/\sqrt{EM}$ for which the results have been presented comprise the full range of relevance. The estimate of the face sheet buckling condition for the tetragonal truss core is more accurate than in the earlier study (Wicks and Hutchinson, 2001). However, there is little difference between the earlier results and those presented here. As before, the full honeycomb optimization results in plate thickness H_c of more than 0.10ℓ which is unrealistically thick. Here optimal results are shown both for the case where H_c/ℓ for the honeycomb core is constrained to be less than 0.10 and where H_c/ℓ is constrained to be identical to that of the optimal tetragonal core structure at the same $V/\sqrt{EM}$. Thus, with no crushing stress, the optimal honeycomb core structure is the lighter weight design, over the entire range of transverse shear load parameter, although the relative advantage is not large especially when the two cores have the same thickness.

In Fig. 8b the crushing strength of these optimal structures are plotted. Clearly the optimal tetragonal core structure is far superior in this regard. Indeed, it is seen that the honeycomb core is unusually vulnerable to crushing. The superiority of the tetragonal core is due to two effects—its inherent advantage at low densities, as illustrated in Fig. 7b and the fact that the optimal tetragonal
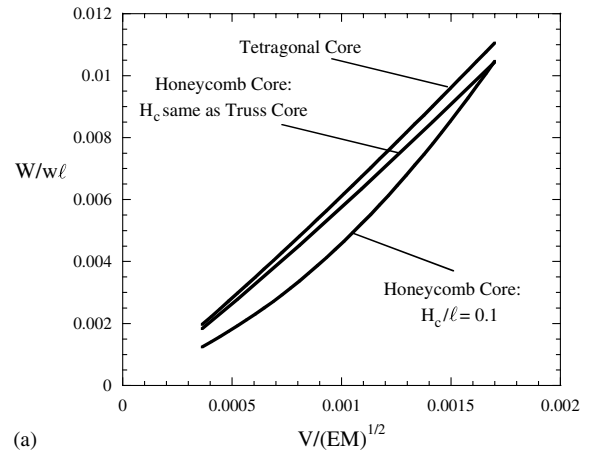
(a)
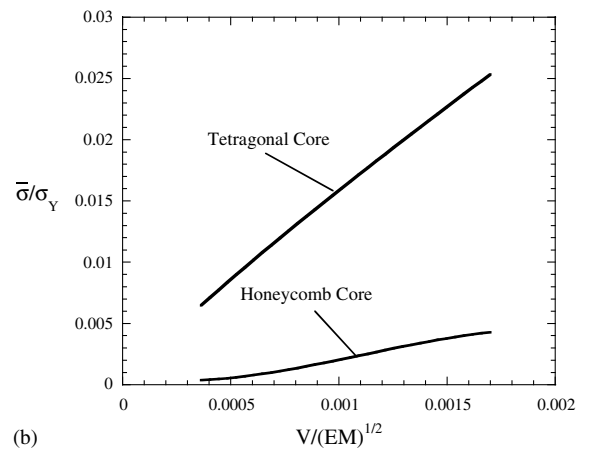
(b)

Fig. 8. Normalized weight per unit area of optimized tetragonal and honeycomb core sandwich panels subject to transverse shear and moment (a). Two cases of honeycomb panels have been considered: the core thickness fixed at $H_c/\ell = 0.1$; and the core thickness taken equal to that of the sandwich plate with truss core at the same value of $V/\sqrt{EM}$. Crushing strength of the optimized tetragonal and honeycomb core structures (b). The honeycomb panel results are for the core thickness fixed at $H_c/\ell = 0.1$ ($\varepsilon_Y = 0.007$).

core plate has somewhat higher core density than the optimized honeycomb core plate.

4.3. Optimization with a crushing stress constraint

To illustrate the effect of the crushing stress constraints, the optimization was run at a midrange load combination corresponding to $V/\sqrt{EM} = 0.001$, over a range of crushing stress from
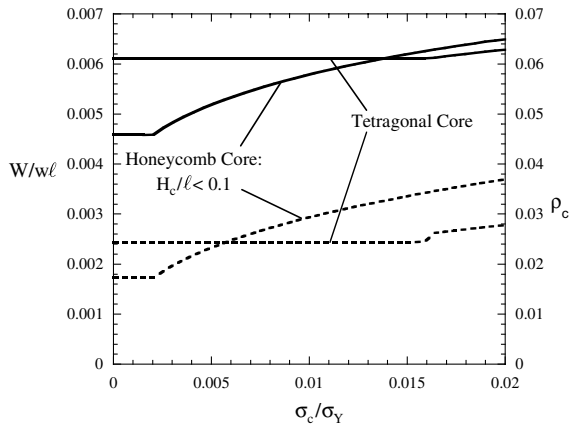
Fig. 9. Top solid lines are minimum weights for tetragonal and honeycomb core structures subject to crushing stress as well as normalized transverse load value $V/\sqrt{EM} = 0.001$. Bottom dashed lines are the core relative densities for these optimized structures ($\varepsilon_Y = 0.007$).

0% to 2% of the material yield stress, σ_Y. The results from this optimization are shown in Fig. 9. Both the minimum weight and the core relative densities are plotted. At the higher values of prescribed crushing stress (above about 1.4% of the material yield stress), the optimized tetragonal core is the lighter of the two structures. The honeycomb structure has a higher core density at the higher levels of crushing stress in order to counteract its inferior crushing resistance properties.

For the tetragonal core structures, face member yield and buckle are active constraints throughout the load range plotted. At low values of crushing stress (below about 1.5% of the yield stress), core member buckle (from the transverse loads) is an active constraint. At higher values of crushing stress, core member crush buckling becomes active. The core members of the optimized tetragonal core have $H_c > \sqrt{2/3}L_c$ corresponding to members oriented closer to the perpendicular to the face sheet than is the case for a regular tetrahedron. This orientation increases both the crushing strength of the core and the ability of the core to resist face sheet buckling (by decreasing the wavelength of the buckle).

The full honeycomb optimization results in plate thickness H_c of more than 0.10ℓ over the low end of the loading range. This is not a thin plate

and such a design would most likely not be considered in an application. In order to make a meaningful comparison between the plates with honeycomb and truss cores, H_c/ℓ for the honeycomb was constrained to be less than 0.10 over the entire optimization. With no crushing stress, the active constraints for the honeycomb plate are face yield, face buckle, and core web buckle. Above low levels of crushing stress (as low as 0.2% of the yield stress), the active constraints switch to face yield and core member crush buckling. These constraints remain active throughout the higher crushing stress levels shown in Fig. 9.

One final optimization comparison is shown in Fig. 10. In this example, the crushing stress is fixed at 2% of the yield stress of the material, while the $V/\sqrt{EM}$ load combination varies over the same range previously plotted. In the presence of this crushing stress, the optimal tetragonal core structure is actually lighter than the optimal honeycomb core structure over the entire range plotted, although the difference between the weights of the two designs is small. A design constraint requiring a crushing strength of 2% of the base material yield stress is not unreasonable. Constraints for certain applications might dictate even larger crushing strengths.
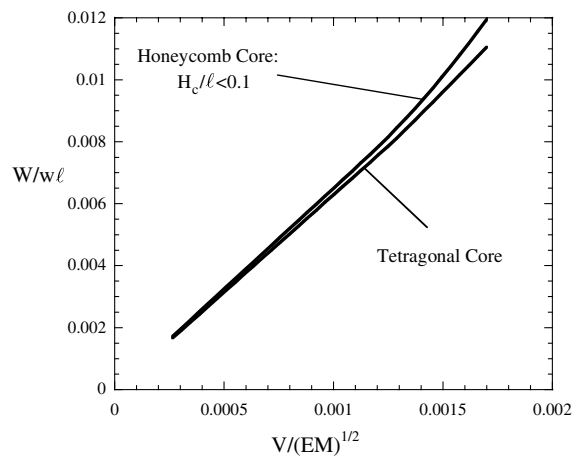
Fig. 10. Normalized weight per unit area of optimized tetragonal and honeycomb core sandwich panels subject to a crushing stress of $\sigma_c/\sigma_Y = 0.02$, as well as transverse shear and moment. Here the honeycomb core thickness has been constrained such that $H_c/\ell \leqslant 0.1$ ($\varepsilon_Y = 0.007$).

5. Conclusions

Truss core construction appears to be as efficient as honeycomb core construction for sandwich plates optimally designed to carry prescribed combinations of moment and transverse force when a realistic minimum crushing strength is imposed. If the constraint on the crushing strength is relaxed, optimized honeycomb core plates have a slight weight advantage, but their crushing strength is exceptionally low. By contrast, the truss core has an inherent crushing advantage at the low core densities typical of most sandwich plate designs. It is this advantage that wins the day when a design constraint on crushing strength becomes important. Given the very close competition between the two methods of construction from a weight perspective, the advantage outcome is likely to hinge on other issues such as ease of manufacture, vulnerability to delamination or moisture, and multifunctional capabilities. In each of these categories, truss core sandwich construction has distinct possibilities that may tilt the advantage in its favor.

Acknowledgements

Appendix A. Bifurcation buckling analysis of the planar truss under pure moment

Fig. 11 shows the unit cell for the finite difference analysis. In the *j*th cell, there are two types of nodes and four types of members. The force and displacement quantities are expanded in perturbation series about the pre-buckling state in the usual way i.e. $N_j^3 = -P + \xi \widetilde{N}_j^3 + \cdots$, $N_j^4 = P + \xi \widetilde{N}_j^4 + \cdots$, $w_j^k = \xi \widetilde{w}_j^k + \cdots$, etc. The six equations of perturbed nodal equilibrium (force balance in two directions and moment balance, at each node type) can then be written in matrix form:
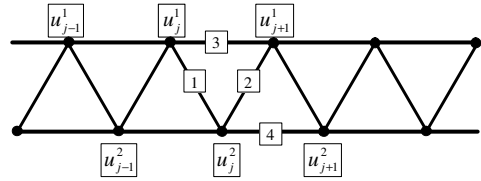
Fig. 11. Unit cell for exact 2D finite difference buckling analysis.

$$K_{ij}F_j = 0$$

where $\vec{F}$ is a vector of the 22 force-like quantities which enter into the perturbed equilibrium equations. (N_j^k, V_j^k, M_j^k are the axial force, shear force, and moment respectively in the *k*th member of the *j*th unit and u_j^k, w_j^k, θ_j^k are the displacements and rotation of the *k*th type node of the *j*th unit.) Thus, K is a 6 by 22 matrix.

Treating each member as a beam column, the force quantities are related to the displacement components and rotations at the ends of the members:

$$F_i = B_{ij}U_j$$

where $\vec{U}$ is a vector of the 18 displacements and rotations at the *j*th joints and the joints adjacent to these joints. B is a 22 by 18 matrix relating these quantities. These relations for a beam of length L with a compressive axial force P are:

$$N(0) = N(L) = -\frac{EA}{L}[u(L) - u(0)]$$

$$M(0) = -\frac{2EI}{L}\left[2C_{10}\theta(0) + C_{20}\theta(L) - \frac{3C_{30}}{L}(w(L) - w(0))\right]$$

$$M(L) = \frac{2EI}{L}\left[2C_{10}\theta(L) + C_{20}\theta(0) - \frac{3C_{30}}{L}(w(L) - w(0))\right]$$

$$V(0) = V(L)$$

$$= \frac{6EI}{L^2}\left[C_{30}(\theta(0) + \theta(L)) - \frac{2C_{40}}{L}(w(L) - w(0))\right]$$

where A is the member cross-sectional area and C_{10}, C_{20}, C_{30}, and C_{40} are the stability functions (Bleich, 1952) defined as:

$$C_{10} = \frac{\overline{P}(\sin\overline{P} - \overline{P}\cos\overline{P})}{4(2 - 2\cos\overline{P} - \overline{P}\sin\overline{P})}$$

$$C_{30} = \frac{\overline{P}^2(1 - \cos\overline{P})}{6(2 - 2\cos\overline{P} - \overline{P}\sin\overline{P})}$$

$$C_{20} = \frac{\overline{P}(\overline{P} - \sin\overline{P})}{2(2 - 2\cos\overline{P} - \overline{P}\sin\overline{P})}$$

$$C_{40} = \frac{\overline{P}^3\sin\overline{P}}{12(2 - 2\cos\overline{P} - \overline{P}\sin\overline{P})}$$

where $\overline{P} = (PL^2/EI)^{1/2}$ is the dimensionless load parameter used in the beam analysis. These relations can be analytically continued to cases with tensile or zero axial load.

Solutions are assumed of the periodic form $u_j^1 = e^{i\mu j}C_1$, $w_j^1 = e^{i\mu j}C_2$, etc. Displacement quantities are then expressed as:

$$U_k = e^{i\mu j}D_{km}C_m$$

where the C_m are six complex constants that determine the buckling mode. The set of equilibrium equations can then be written:

$$K_{ij}B_{jk}D_{km}C_m = 0$$

In order to find bifurcation solutions, the matrix $K_{ij}B_{jk}D_{km}$ must be singular. In dimensionless form, this matrix is a function of the dimensionless quantities μ, R_{f}/L, R_{c}/L, and M/EL^3. Physically, these quantities are the wave-number of the peri-odic solution, the slenderness ratios of the horizontal and core members, and the dimensionless buckling moment (the eigenvalue of the system).

Computations were performed to calculate the lowest eigenvalue (M/EL^3) for a given set of ($\mu, R_{\mathrm{f}}/L, R_{\mathrm{c}}/L$). The determinant of the matrix is non-negative, dropping to zero at the eigenvalues and then increasing again. This is due to the fact that in this complex formulation the eigenvalues are double-roots. In the numerical computations, the eigenvalues were found by looking for zero-crossings of the derivative of the matrix determinant.

References

Bleich, F., 1952. Buckling Strength of Metal Structures. McGraw-Hill, New York. pp. 210–211.

Brittain, S., Sugimura, Y., Schueller, O.J.A., Evans, A.G., Whitesides, G.M., 2001. Fabrication and mechanical performance of a mesoscale, space-filling truss system. JMEMS 10, 113–120.

Evans, A.G., Hutchinson, J.W., Fleck, N.A., Ashby, M.F., Wadley, H.N.G., 2001. The topological design of multifunctional cellular metals. Progress in Materials Science 46, 309–327.

Wicks, N., Hutchinson, J.W., 2001. Optimal truss plates. International Journal of Solids and Structures 38, 5165–5183.